Environmental Science and Pollution Research
https://doi.org/10.1007/s11356-022-21037-9

RESEARCH ARTICLE

Urban ventilation corridors and spatiotemporal divergence patterns of urban heat island intensity: a local climate zone perspective

Zhipeng Shi[1] · Jun Yang[1,2] · Yuqing Zhang[1] · Xiangming Xiao[3] · Jianhong Cecilia Xia[4]

Received: 6 April 2022 / Accepted: 19 May 2022

Abstract
Urban ventilation corridors introduce fresh air into urban interiors and improve urban livability, while mitigating the urban heat island (UHI) effect. However, few studies have assessed the impact of urban ventilation corridors on UHI intensity (UHII) from the perspective of the local climates of different cities. Therefore, this study integrated multisource data to construct ventilation corridors from the perspective of local climate zone (LCZ) and analyzed its impact on UHII. The results showed the following: (1) the average UHII of constructed LCZs was higher than that of natural LCZs, among which the building type LCZ10 (heavy industry) had the highest intensity (5.77 °C); (2) in extracted ventilation corridors, the pixel number of natural LCZs was substantially larger than that of constructed LCZs, among which LCZE (bare soil/paved) was the largest; and (3) for natural LCZs, the average UHII of each LCZ was lower within the ventilated corridors than within the non-ventilated corridors (except for LCZG [water]), with the UHII of LCZB (scattered trees) exhibiting the greatest mitigation effect. Quantitative research on the composition and function of ventilation corridors can not only assess the ability of ventilation corridors to mitigate UHIs, but also provide a reference for urban ventilation corridor planning.

Keywords Ventilation corridors · Local climate zones · Frontal area index · Urban heat island · Land surface temperature · Dalian City

Responsible Editor: Philippe Garrigues

✉ Jun Yang
yangjun8@mail.neu.edu.cn

Zhipeng Shi
shizhipeng_gis@163.com

Yuqing Zhang
zhangyuqing@lnnu.edu.cn

Xiangming Xiao
xiangming.xiao@ou.edu

Jianhong Cecilia Xia
c.xia@curtin.edu.au

1 Human Settlements Research Center, Liaoning Normal University, Dalian 116029, China

2 Jangho Architecture College, Northeastern University, Shenyang 110169, China

3 Department of Microbiology and Plant Biology, Center for Earth Observation and Modeling, University of Oklahoma, OK 73019 Norman, USA

4 School of Earth and Planetary Sciences (EPS), Curtin University, Perth 65630, Australia

Introduction

According to the United Nations, the global population is expected to reach 9.7 billion by 2050, with 68% of people living in urban areas (2019) (DESA 2019). However, urban areas only cover approximately 1% of the Earth's surface (Schreurs 2008). Rapid growth of urban populations and limited urban spaces have led to compact and high-density architectural layouts in most cities (Ngarambe et al. 2021). This architectural model has increased the roughness of the underlying ground surface and reduced urban wind speed, leading to urban problems such as air pollution, urban heat island (UHI) formation, and increased energy consumption (Giridharan et al. 2004; Shi et al. 2021; Roxon et al. 2020). Therefore, understanding and improving urban ventilation is crucial not only for enhancing the self-purification ability of urban air and improving air quality, but also for mitigating the UHI effect and improving the comfort of urban residents (Luo et al. 2021; Ren et al. 2022).

With the development of remote sensing technology and geographical information systems (GIS), numerous studies have analyzed the surface UHI effect using remote sensing

Published online: 30 May 2022

data (Min et al. 2018; Zhang and Cheng 2019; Athukorala and Murayama 2021; Yang et al. 2021). UHIs can be categorized into subsurface, surface, canopy layer, and boundary layer UHIs (Oke et al. 2017). Owing to the limited distribution of weather stations, remote sensing data are more typically used for UHI studies than are air temperature data. Related studies include those focused on the spatiotemporal distribution, driving mechanisms, and mitigation measures of the UHI effect (Jun et al. 2021; Athukorala and Murayama 2021). Research on UHI has been conducted at three scales: macro, meso, and micro (Berger et al. 2017; Jiang et al. 2020; Qiquan et al. 2021; Tian et al. 2021). For example, Yang et al. (2020) studied the Pearl River Delta urban agglomeration from a regional perspective and found that the temperature within the city presented a conspicuous hierarchical effect at different city scales. Furthermore, UHI intensity (UHII) can effectively quantify the UHI effect, and the spatiotemporal distribution of UHIIs can reasonably reflect the developmental trends of cities (George et al. 2021; Li et al. 2021b; Wang et al. 2021). Quantitative research on the spatial differences of UHII from a local perspective assists not only in providing a reference for urban construction but also in formulating corresponding strategies.

Rapid land-use change is due to economic development and urbanization factors (Li et al. 2018).Numerous studies have revealed that urban water bodies and vegetation can effectively mitigate the UHI effect (Qiao et al. 2013; Tan et al. 2016; He 2018; Jamei et al. 2020; Ma et al. 2021). In addition, good urban ventilation is reportedly effective in alleviating UHIs (Xu et al. 2021). Accordingly, urban ventilation is considered a core part of the urban climate. At present, research methods for urban ventilation environments primarily include the field test, wind tunnel test, and numerical simulation methods (Hou et al. 2018; Qin et al. 2020; Yunlong et al. 2021). Buccolieri and Hang (2019), Franchesca et al. (2019), and Coccia (2021) have evaluated the performance of urban ventilation by calculating various indicators (wind speed, age of air, and wind speed ratio, respectively). Similarly, Peng et al. (2019) calculated air velocity, mean age of air, purification velocity, and six other indicators to evaluate local ventilation performance and further analyzed the quantitative relationships among urban ventilation, floor area ratio, and construction site coverage . Fang et al. (2021) and Xu et al. (2017) constructed urban ventilation corridors by calculating urban building form parameters or surface roughness to introduce suburban fresh air into the city interior and alleviate the urban high-temperature phenomenon. Among these parameters, the frontal area index (FAI) is considered a highly accurate indicator of roughness and has been widely used in the study of urban ventilation corridors (Chen et al. 2017; Qiao et al. 2017). Based on the calculation of FAI, Guo et al. (2018) and Liu et al. (2021) used the least cost path (LCP) method to construct urban ventilation corridors and analyze the impact of ventilation corridors on the urban thermal environment (Guo et al. 2018; Liu et al. 2021). LCPs are widely used in the construction of urban ventilation corridors owing to their speed and accuracy in identifying the least expensive path between the source and end point.

Owing to rapid urbanization, the internal architecture of cities has become increasingly complex, resulting in considerable differences in urban ventilation. Therefore, applying the concept of zoning is necessary while conducting research on urban ventilation. He et al. (2020) proposed a scheme for zoning ventilation areas and applied it to study the ventilation performance of open mid-rise street structures in Sydney, Australia. In addition, the local climate zone (LCZ) classification scheme has been proposed for UHIs for application in urban wind environments (Zhao et al. 2020). The LCZ classification divides the underlying surface of the city into different types based on differences in surface material and structure. While two-dimensional elements are considered, the three-dimensional spatial elements are emphasized (Li et al. 2021a). Therefore, LCZ schemes can accurately describe the influence of urban morphology on the UHI effect. Yang et al. (2019a) investigated the FAI of different LCZs in China to evaluate the ventilation performance of the different zones of Shanghai and the influence of season on the surface temperature. Moreover, Zhao et al. (2020)using Shenyang as a research area revealed that LCZ classification can be applied to study urban ventilation performance at the local scale. In summary, urban ventilation corridors could effectively alleviate the UHI effect. However, existing studies have focused mostly on exploring the effects of urban ventilation corridors and less on the specific analysis of their composition.

Therefore, the major aims of this study were to (1) construct urban ventilation corridors through the LCP algorithm based on weather and building data and simultaneously calculate building height and building density, to be combined with land-use data for LCZ division; (2) calculate UHII to quantify UHI characteristics using remote sensing image data; and (3) use GIS spatial analysis technology to superimpose the ventilation corridors and LCZ layers, discuss their composition from the perspective of LCZ, and analyze the influence of different LCZ types on UHII.

Materials and methods

Study area and research data

Dalian City is located between 38°43′–40°12′N and 120°58′–123°31′E. Its terrain is primarily mountainous and hilly, and the region receives concentrated rainfall and has a distinct monsoon season. The city covers approximately 12,574 km^2, of which the urban area comprises 2,414.96 km^2. The main urban area of Dalian City was selected as the study area (Fig. 1).

The data sources used in this study for building, meteorological, and land-use information are presented in Table 1. The building vector data include the number of floors and the height, which were used for the classification of constructed LCZ types, and the calculation of the FAI. Multi-year wind frequency and direction data were used to determine the dominant wind direction in the study area. Natural LCZ was classified using land-use data, and Landsat-8 data were primarily used to verify the impact of various LCZ types of ventilation corridors on the UHII.

Methods

We integrated multisource data gathered from meteorological stations and Landsat-8 images to analyze the impact of urban ventilation. We also performed LCZ segmentation based on building height and density and analyzed the impact of urban ventilation corridors on UHII in different LCZ contexts at a scale of 30 × 30 m. The overall framework and the major data processing methods are presented in Fig. 2.

LCZ classifications

The impact of different landscape types on urban climate varies greatly. Additionally, the architecture and spatial

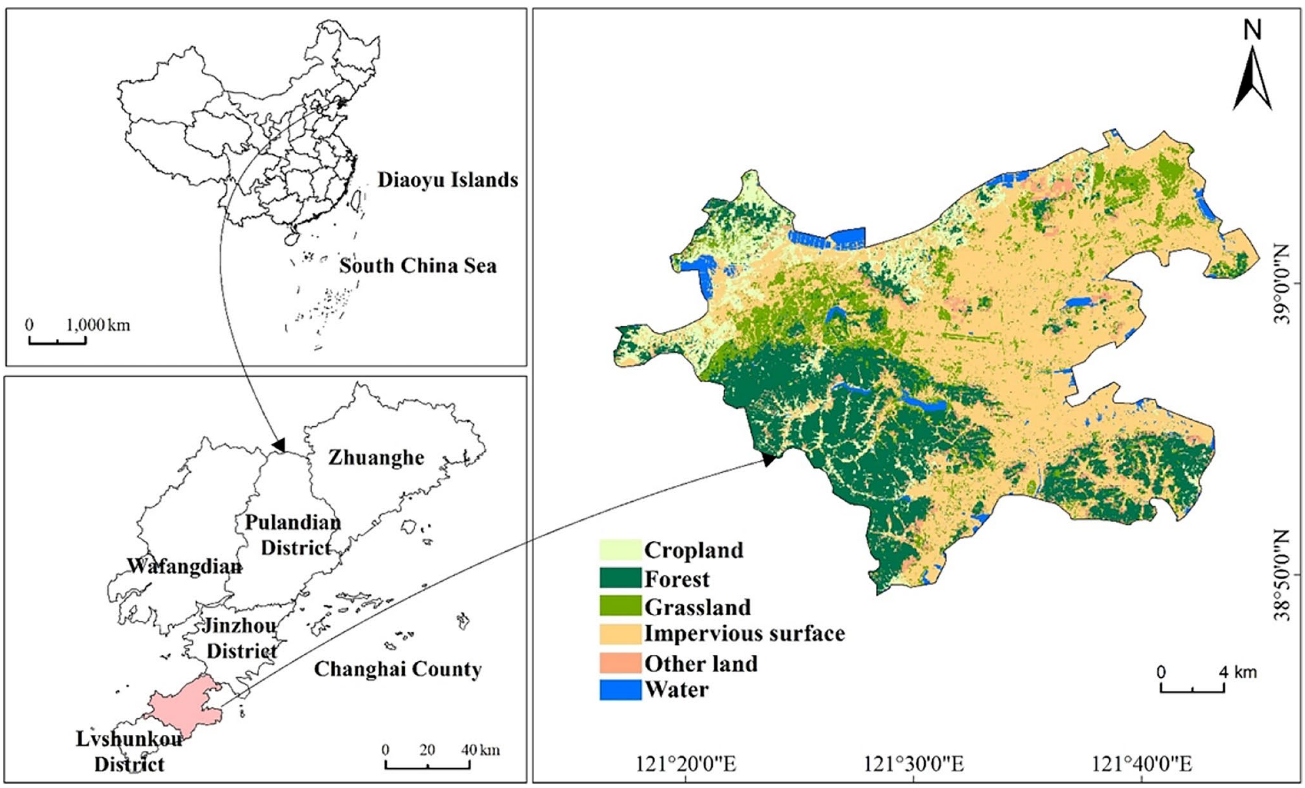

Fig. 1 Location of the main urban area of Dalian City

Table 1 Data sources and corresponding descriptions

Data	Time	Resolution	Data sources
Building data	2018	Buildings outlines, height and floor	Baidu Map
Meteorological data (wind speed, wind directions, air temperature)	2011–2018	Daily data from 2011 to 2018	China Meteorological Data Network (http://data.cma.cn/)
Landsat-8 (122/33)	2018.8.9 (02:34:29)	OLI 30 m/TIRS 100 m	http://www.gscloud.cn/
Land-use data	2017	10 m	http://data.ess.tsinghua.edu.cn/

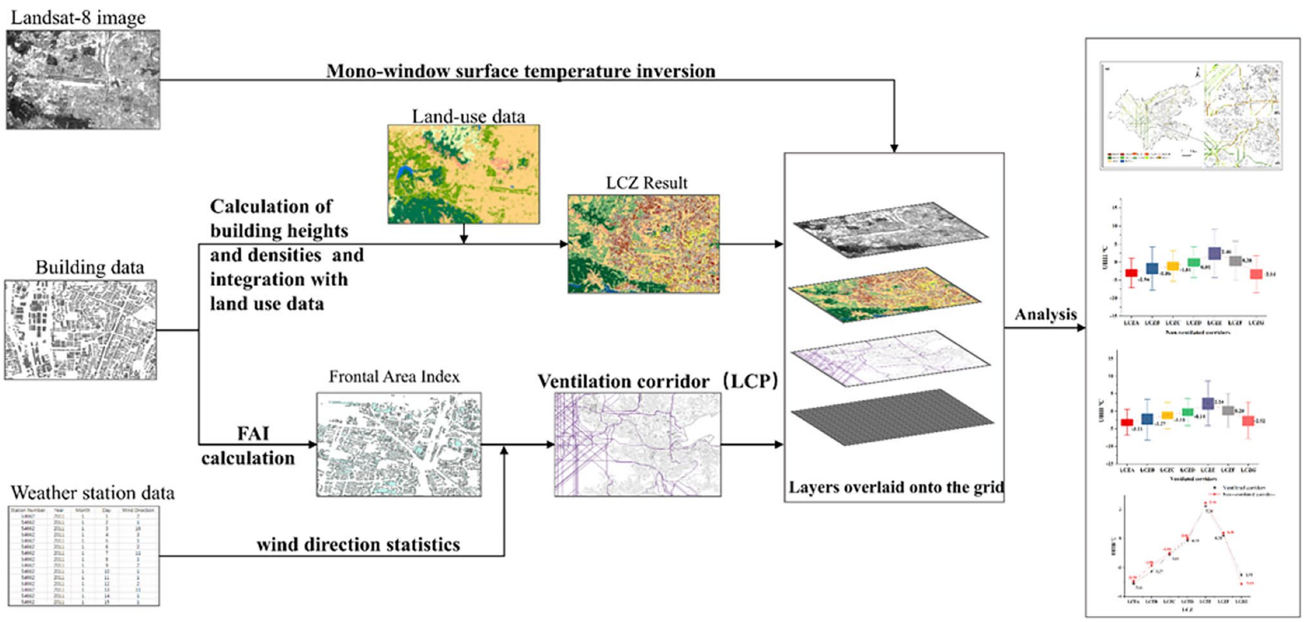

Fig. 2 Research framework and data processing

layout of a city's interiors can cause local climate changes. Therefore, this study was conducted based on local urban climate categories or zones (Stewart and Oke 2012). Correspondingly, the LCZs of the entire study area were categorized into nine architectural types (LCZ1–LCZ9 according to the building height and density). Factories were categorized as LCZ10 according to building function and seven natural types (LCZA–LCZG according to the land-use type) (Table 2). Finally, the two types of LCZs were merged to generate a local climate classification map.

Calculation of urban heat island intensity

The urban thermal environment interacts with the wind environment, and the urban heat island intensity (UHII) can be used to visualize the condition of the urban thermal environment. The traditional UHII calculation is usually based on the temperature difference between urban and rural areas; however, this method has certain shortcomings, especially in the definition of urban and rural areas. Moreover, the limited temperature data from meteorological stations do not generally reflect the thermal environment conditions of the whole city; in addition, it is difficult to uniformly evaluate UHIs in different cities. Therefore, to provide a comprehensive view of the effect of ventilation on the UHI effect, this study used the Stewart and Oke (2012) definition of UHII, which is the temperature difference between each LCZ type and that of the specific natural LCZ type, LCZD (low plants). The calculation formula is as follows:

$$\mathrm{UHII}_{\mathrm{LCZX}} = \mathrm{T}_{\mathrm{LCZX}} - \mathrm{T}_{\mathrm{LCZD}} \tag{1}$$

where $\mathrm{UHII}_{\mathrm{LCZX}}$ is the UHII of LCZX (℃), T_{LCZX} is the temperature of LCZX (℃), and T_{LCZD} is the average temperature of LCZD (℃).

To maintain the consistency of the grid scale and accuracy of the data, a Landsat-8 remote sensing image with < 5% cloud cover was selected, and the mono-window algorithm of Qin et al. was used to retrieve the land surface temperature (Qin et al. 2001). The calculation formulas are as follows:

$$T\_s = (a(1 - C - D) + (b(1 - C - D) + C + D)T\_10 - DT\_a)/(C - 273.15) \tag{2}$$

$$\mathrm{C} = \varepsilon\tau \tag{3}$$

$$\mathrm{D} = (1 - \tau)[1 + (1 - \varepsilon)\tau] \tag{4}$$

where $T_{\_S}$ is the surface temperature value obtained by inversion (K); $T_{\_a}$ is the average temperature of the atmosphere (K); $T_{\_10}$ is the brightness temperature (K) of the sensor; a and b are reference coefficients (when the surface temperature is between 0 and − 70 °C, a = −67.355351, b = 0.458606); τ is the atmospheric transmittance; and ε is the surface emissivity.

Construction of the urban ventilation corridor

Surface roughness is an important factor affecting urban ventilation, and FAI is considered one of the most accurate

Table 2 LCZ types and description

LCZ Type	Description	Examples	LCZ Type	Description	Examples
LCZ1	Compact high-rise (more than 9 floors)		LCZA (Dense trees)	Dense coniferous forest and evergreen forest.	
LCZ2	Compact mid-rise (4–8 floors)		LCZB (Scattered trees)	Sparse coniferous forest and evergreen forest.	
LCZ3	Compact low-rise (1–3 floors)		LCZC (Shrub)	Open arrangement of bushes, shrubs, and short, woody trees.	
LCZ4	Open high-rise (more than 9 floors)		LCZD (Low plants)	Grassland or herbaceous plants crops. Few or no trees.	
LCZ5	Open mid-rise (4– 8 floors)		LCZE (Bare soil or paved)	Rock or impervious road surface virtually vegetation free	
LCZ6	Open low-rise (1–3 floors)	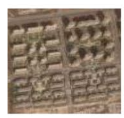	LCZF (Bare soil or sand)	Featureless landscape of soil or sand cover. Few or no trees or plants.	
LCZ7	Sparse high-rise (more than 9 floors)		LCZG (Water)	Large, open water bodies or small bodies.	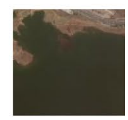
LCZ8	Sparse mid-rise (4– 8 floors)				
LCZ9	Sparse low-rise (1– 3 floors)			LCZ1–3: building density greater than 0.4. LCZ4–6: building density is between 0.2 and 0.4. LCZ7–9: building density less than 0.2.	
LCZ10	Heavy industry				

indicators of roughness (Liu et al. 2016). FAI is defined as the ratio of the sum of the projected area of a horizontal unit of building area to the unit's horizontal area for a given wind direction. The calculation formula is as follows:

$$\lambda_{f(\theta)} = \frac{A_{F(\theta)} Z_{meanT}}{A_T} \tag{5}$$

where θ is the wind direction, $\lambda_{f(\theta)}$ is the FAI corresponding to the θ wind direction, $A_{F(\theta)}$ is the projected area on the θ wind direction, A_T is the horizontal bottom area (m^2), and Z_{meanT} is the average height of the unit grid (m). The FAI of each wind direction in this study was calculated via programming.

The LCP method was used to determine potential ventilation corridors. This method finds a path with the lowest cost between the start point and end point (Wong et al. 2010). In this study, the calculated FAI value was used as the cost value; the starting point and end point were set according to the wind direction and frequency data, and 16 wind directions were constructed. Finally, the ventilation paths of each wind direction were superimposed to obtain the overall ventilation corridor.

Results

LCZ classification results

Referring to the local climate division standard, the building height and density in the grid were used to classify the buildings, merge them with the land-use data, and finally implement the results into a 30 × 30 m grid to obtain the main urban area of the city's local climate map (Fig. 3) (Yang et al. 2019b). The results showed that the entire study area can be divided into 670,716 pixels (Fig. 4), of which constructed LCZs accounted for 160,237 (~ 24% of the total), and natural LCZs accounted for 510,179 pixels (76%). Among the constructed LCZs, LCZ9 (sparse low-rise) had the largest number of pixels (32,382), followed by LCZ8 (sparse mid-rise; 30,386 pixels) and LCZ5 (open mid-rise; 24,928 pixels). LCZ10 (heavy industry) had the least pixels (2086). Among the natural LCZs, LCZE (bare soil/paved) had the largest number of pixels (174,634), followed by LCZA (dense trees; 141,015 pixels) and LCZD (130,645 pixels).

UHII results

In terms of spatial distribution, the UHII exhibited higher distribution in four districts of the study area: the eastern parts of Ganjingzi district, and the northern part of the Zhongshan, Xigang, and Shahekou districts (Fig. 5). The spatial autocorrelation analysis of the UHII revealed that the global spatial autocorrelation coefficient (Moran's I) had a value of 0.99, indicating that the UHII exhibited a strong positive spatial correlation. From the perspective of LCZ (Fig. 3), the northeastern part of the study area was primarily composed of constructed LCZs; therefore, the UHII in that region was strong. However, the western part of the study area primarily comprised natural LCZs, with limited constructed LCZs. As shown in Table 3, the overall average UHII of the constructed LCZs was greater than 0 °C, and the average UHII of LCZ10 (Heavy industry) was the highest (5.77 °C). For natural LCZs, the UHI strength was generally less than 0 °C, except for LCZE and LCZF (bare soil/sand). This is because LCZA and LCZD, as well as LCZB (scattered trees), LCZC (shrub), and LCZG (water), primarily comprised vegetation and water bodies, and hence, their temperatures and corresponding UHII values were low. In contrast, LCZE and LCZF comprised bare rock, pavement, sand, and soil. These materials have a higher heat absorption rate and a low heat capacity (Mohajerani et al. 2017); therefore, its corresponding LCZ type exhibited a high UHII.

LCZ and ventilation corridors

Ventilation corridor construction

We extracted the entire-year temperature data of the Dalian Meteorological Station from 2011 to 2018 and observed the monthly trends (Fig. 6a). Evidently, the highest temperatures occurred in August (30.7 °C), followed by July and June. Therefore, we defined June, July, and August as summer and simultaneously obtained the wind frequency and direction data of the corresponding months, thereby producing a wind rose of the study area (Fig. 6b). Four wind directions (south, south–southwest, north, and southwest) prevailed during the summer in the study area, with a total frequency of 0.66. We referred to the wind frequency and direction data, based on the FAI cost surface under different wind directions, to construct an urban ventilation corridor map for the study area (Fig. 7). Unlike the traditional construction of ventilation corridors, this study did not count the frequency of occurrence of ventilation corridors on the grid but obtained the number and spatial locations of ventilation corridors. Consequently, 41,300 pixels were extracted from the constructed ventilation corridor.

Relationship between LCZ and ventilation corridors

The constructed ventilation corridor and LCZ classification map were superimposed, and the LCZ types corresponding to each ventilation corridor were extracted. The different colors in Fig. 8 represent the LCZ type corresponding to each pixel in the ventilation corridor. Table 4 shows the types and numbers of LCZs that constitute the ventilation corridors. Among them, constructed LCZs had a total of 34 pixels, and natural LCZs had a total of 41,266 pixels. From the largest to smallest pixel number, the natural LCZs were ranked as follows: LCZE, LCZA, LCZD, LCZF, LCZG, LCZB, and LCZC. This was possibly because in the highly heterogeneous cities, natural LCZs had a lower average height than constructed LCZs, thereby having less resistance to wind and a larger ventilation potential. In addition to buildings, most of the

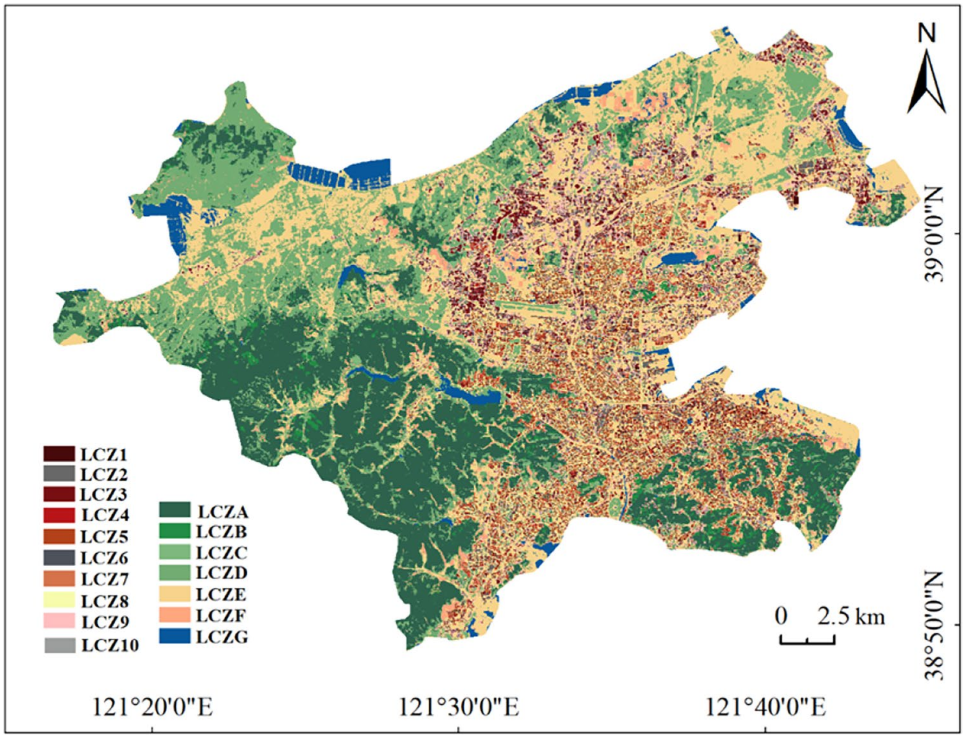

Fig. 3 Urban local climate zone (LCZ) map of the study area

interior of the city was covered by impervious surfaces, of which roads are an important factor. This explains why the largest number of LCZE pixels is in the extracted ventilation corridors.

Discussion

Application of the LCZ classification scheme in the urban wind environment

Zhao et al. (2020) and Zhang et al. (2021) have demonstrated that the LCZ classification scheme is suitable not only for studying urban thermal environments but also for studying urban ventilation. With increased and rapid urbanization and development, a growing number of cities have considered the construction of ventilation corridors and have applied them to urban planning (Trihamdani et al. 2015; Ren et al. 2018; Eldesoky et al. 2020). From our urban ventilation corridor composition results (Table 4), it is evident that natural LCZs are a critical component of ventilation corridors, particularly LCZE. As this LCZ type primarily comprises bare rock and roads, this result suggests that urban roads are an important component in the construction of ventilation corridors. However, related studies have revealed that although urban roads provide a broad channel for urban ventilation, the composition of the road and orientation of the street will also aggravate the UHI effect to a certain extent, and therefore, it is important to select relatively cool materials for urban road paving (Cao et al. 2015; Ramponi et al. 2015; Mohajerani et al. 2017; Lai et al. 2019).

Influence of the LCZ ventilation corridor on UHII

The construction of ventilation corridors has a considerable mitigating effect on UHIs and urban pollution (Abiye, 2016). However, existing research has primarily focused on the construction of urban ventilation corridors, reflecting only their spatial location, without a quantitative analysis of their composition or internal differences. For example, Liu et al. (2021) analyzed the relationship between the FAI and urban thermal comfort under different buffer zones of ventilation corridors and found that the greater the distance from the urban ventilation corridor, the lower the impact on thermal comfort. However, differences in the urban architectural forms and surface coverage exist even within the same buffer zone, thereby producing different effects on UHIs.

Owing to the small number of constructed LCZs that corresponded with ventilation corridors (Table 4), only the cooling effects of natural LCZs have been discussed herein. Figure 9a shows the average UHII of each LCZ

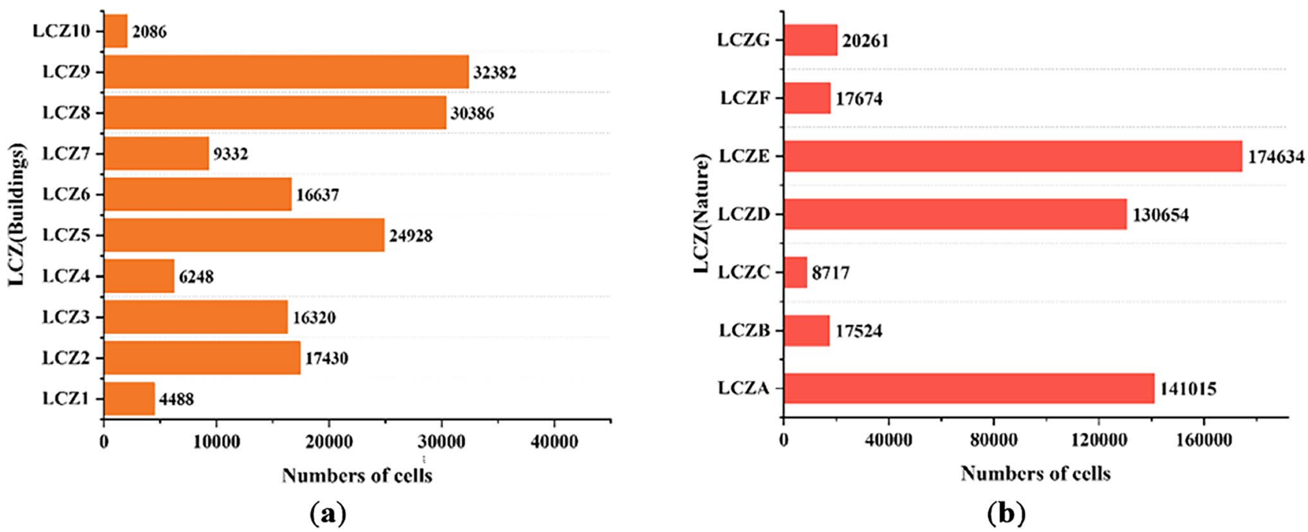

Fig. 4 Number of built and natural-type LCZs in the study area, **a** the number of building type LCZs; **b** the number of nature type LCZs

under the non-ventilated corridor, where LCZE has the highest UHII (2.46 °C), followed by LCZF > LCZD > LCZC > LCZB > LCZA > LCZG. Figure 9b shows the UHII of different LCZs under the ventilated corridors, which also exhibits an overall trend of LCZE > LCZF > LCZD > LCZC > LCZB > LCZA > LCZG. The final comparative results of UHII for ventilated versus non-ventilated urban corridors (Fig. 10) show that the average UHII of each LCZ type within ventilated corridors was generally lower than that of non-ventilated corridors (expect LCZG). Accordingly, natural-type LCZB (scattered trees) had the best alleviation effect on UHIs. Compared with that of the non-ventilated corridors, the average UHII for LCZB was reduced by 0.41 °C, followed by that of LCZE (0.22 °C), LCZF (0.18 °C), LCZA (0.17 °C), LCZD (0.15 °C), LCZC (0.10 °C), and LCZG (– 0.61 °C). Vegetation within the ventilated corridors had a better mitigation effect on UHII, which is

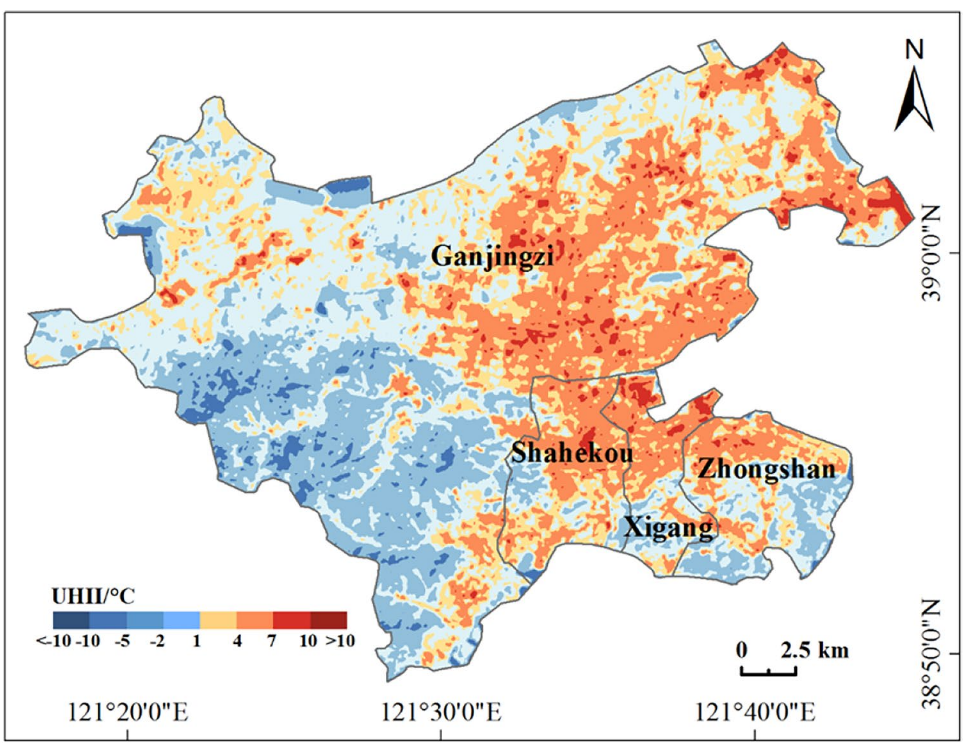

Fig. 5 Distribution of urban heat island intensity (UHII)

Table 3 Statistical results of LCZ type surface temperature (°C)

Built type	Min	Max	Average	Nature type	Min	Max	Average
LCZ1	−3.01	13.91	3.49	LCZA	−9.42	7.22	−2.95
LCZ2	−2.53	16.42	4.50	LCZB	−11.03	8.30	−1.88
LCZ3	−5.34	14.41	4.02	LCZC	−9.86	6.62	−1.02
LCZ4	−3.31	10.91	2.76	LCZD	−10.97	12.85	−0.01
LCZ5	−3.84	13.44	3.95	LCZE	−8.35	14.58	2.45
LCZ6	−4.66	13.67	3.72	LCZF	−9.39	11.19	0.37
LCZ7	−3.35	11.55	2.51	LCZG	−9.83	10.15	−3.10
LCZ8	−3.98	13.22	3.76				
LCZ9	−4.94	13.54	3.34				
LCZ10	−0.41	12.65	5.77				

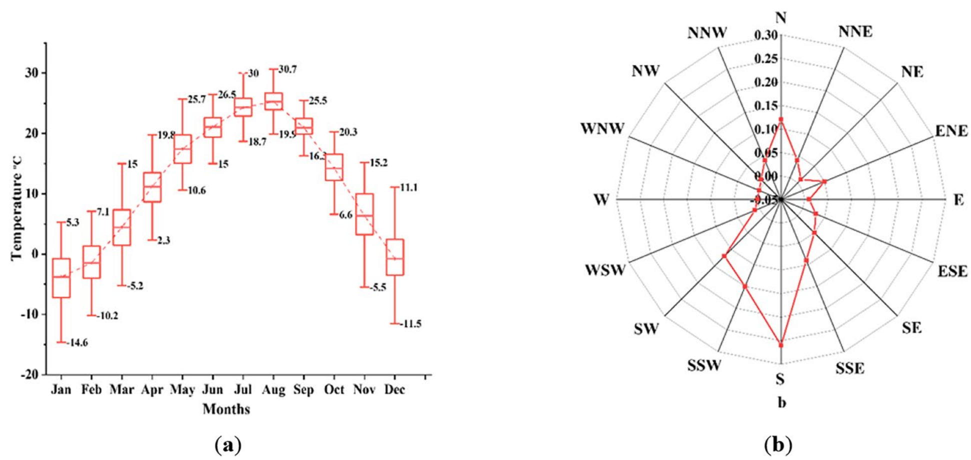

Fig. 6 Box plot of temperature data and wind rose of main urban area of Dalian City from 2011 to 2018. **a** Annual average temperature, and **b** wind rose from June to September

Fig. 7 Results of urban ventilation corridor construction for the main urban area of Dalian City

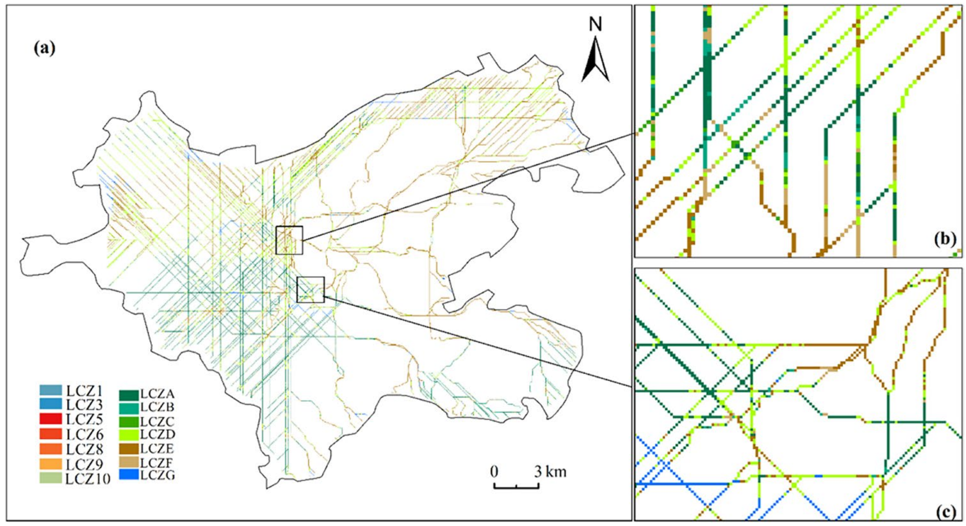

Fig. 8 **a** The different LCZ types corresponding with the ventilation corridors in the entire study area (building types: LCZ1, 3, 5, 6, and 8–10; natural types: LCZA–G; see definitions in Table 2); **b**, **c** the corresponding partial enlargements within the rectangle of (**a**)

Table 4 Number of LCZ type under ventilation corridors

Built types	Numbers (pixels)	Nature types	Numbers (pixels)
LCZ1	1	LCZA	11,420
LCZ3	3	LCZB	1176
LCZ5	1	LCZC	605
LCZ6	2	LCZD	11,231
LCZ8	10	LCZE	13,997
LCZ9	15	LCZF	1588
LCZ10	2	LCZG	1249
Sum	34		41,266

consistent with the results of a previous study (Tan et al. 2016); however, the LCZG within the ventilated corridors did not exhibit a better reduction effect. Combined with the description of each LCZ type in Table 2, Fig. 10 shows that under both the ventilation and non-ventilation corridors, LCZG (water bodies) had the lowest average UHII (− 2.52 °C and − 3.13 °C, respectively). This indicates that compared to other LCZ types, water bodies were more effective in mitigating UHI; however, the average UHII of LCZG (water bodies) under ventilation corridors was higher than that under non-ventilation corridors, which is inconsistent with the findings of other LCZ types. Therefore, future studies should use different methods to construct urban ventilation corridors and further analyze the effect of ventilation on UHI (Xie et al. 2022).

Limitations

Owing to the lack of building outline data, FAI calculation to construct the urban ventilation corridors was only conducted for the existing building area. In subsequent studies, higher resolution images should be used to extract building outline data to improve the calculation accuracy and correspond with the actual ventilation conditions. In addition, this study only calculated the UHII

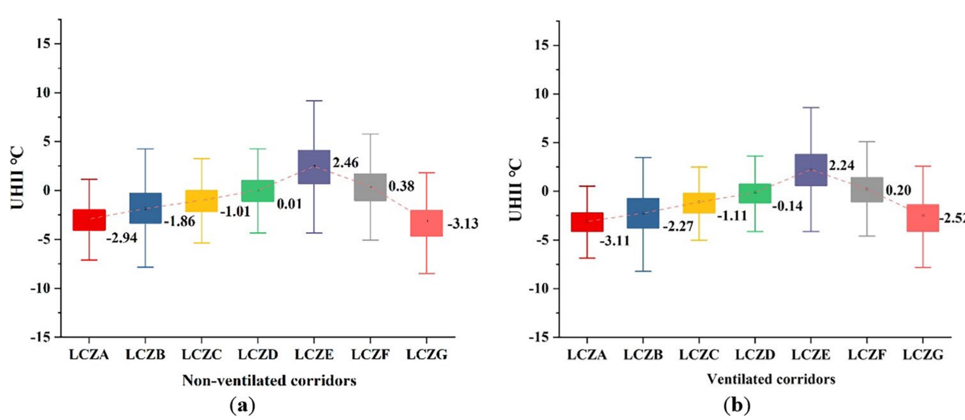

Fig. 9 **a** UHII of the natural LCZs within non-ventilated urban corridors, **b** UHII of the natural LCZs within ventilated urban corridors

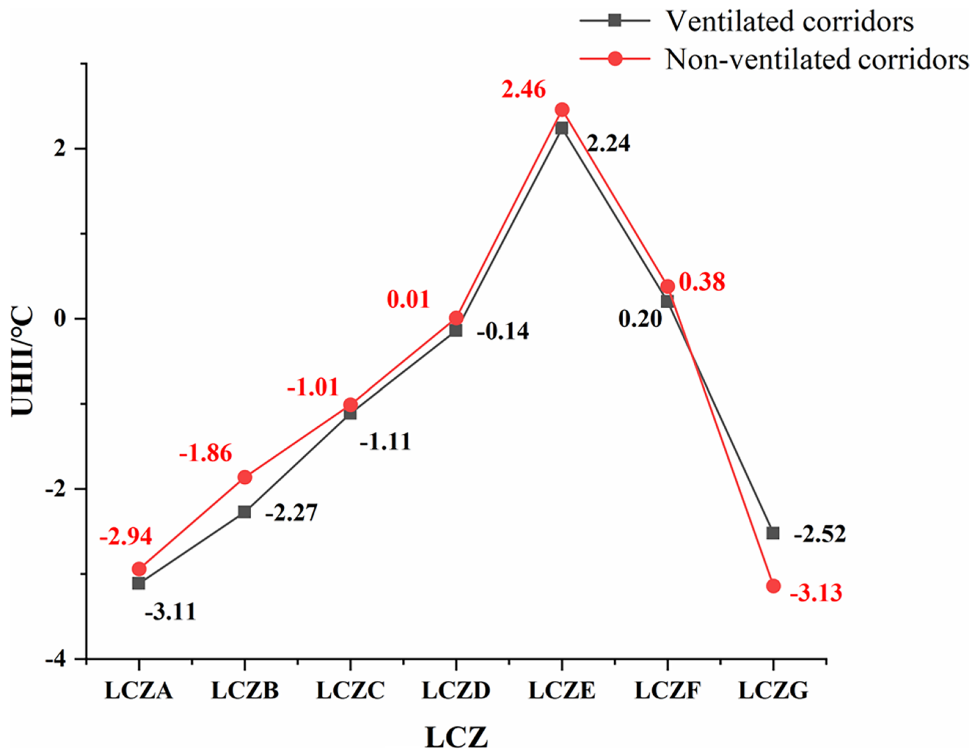

Fig. 10 Average UHII of the natural LCZs within ventilated versus non-ventilated urban corridors

during summer; therefore, subsequent research should analyze the influence of ventilation corridors on UHII both in terms of annual seasonal trends and between daytime and nighttime data.

Conclusions

To obtain a better understanding of the measures to mitigate UHII through constructing urban ventilation corridors and from the perspective of LCZs, this study quantified the impact of urban ventilation corridors on UHII in the main urban area of Dalian City, China, using multisource data. We determined LCZ classification and constructed ventilation corridors using the LCP method. From the LCZ perspective, the urban ventilation corridors and their relationship with UHII were analyzed. The main conclusions are as follows:

The LCZ classification results for the main urban area of Dalian City showed that constructed LCZs (160,237 pixels or 24%) were significantly less than natural-type LCZs (510,179 pixels or 76%). Among the built types, LCZ9 (sparse low-rise) was the most common classification.

The corresponding UHIIs were different for each LCZs type. Among them, constructed type LCZ10 (heavy industry) had the highest average UHII (5.77 °C). Overall, constructed LCZs had higher UHII than natural LCZs.

In total, 41,300 pixels were extracted from the constructed urban ventilation corridors, including 34 pixels for constructed LCZs and 41,266 pixels for natural LCZs. Among the natural LCZs, LCZE (bare soil/paved) had the largest pixel number (13,997 pixels), followed by LCZA, LCZD, LCZF, LCZG, LCZB, and LCZC. Within the ventilation corridors, the different natural LCZ types had varying levels of impact in terms of their mitigating effect on UHII, with LCZB (scattered trees) being the most effective (− 0.40 °C), followed by LCZE (− 0.22 °C) > LCZF (− 0.18 °C) > LCZA (− 0.17 °C) > LCZD (− 0.15 °C) > LCZC (− 0.1 °C). Notably, in this study, LCZG (water) had an unexpectedly poor mitigation effect on UHII. The present findings provide a basis for continuing quantitative research on the composition and effectiveness of urban ventilation corridors for mitigating heat intensity from the LCZ perspective.

Acknowledgements The authors would like to acknowledge all colleagues and friends who have voluntarily reviewed the translation of the survey and the manuscript of this study.

Author contribution Jun Yang contributed to all aspects of this work; Zhipeng Shi wrote the main manuscript text, conducted the experiment, and analyzed the data; Yunqing Zhang, Xiangming Xiao, and Jianhong (Cecilia) Xia revised the paper. All authors reviewed the manuscript.

Funding This research study was supported by the National Natural Science Foundation of China (grant no. 41771178, 42030409), the

Fundamental Research Funds for the Central Universities (grant no. N2111003), Basic Scientific Research Project (Key Project) of the Education Department of Liaoning Province (grant no. LJKZ0964), the Second Tibetan Plateau Scientific Expedition and Research Program (STEP) (grant no. 2019QZKK1004), and Innovative Talents Support Program of Liaoning Province (grant no. LR2017017).

Data availability Not applicable.

Declarations

Ethics approval and consent to participate Not applicable.

Consent to publish Not applicable.

Conflict of interest The authors declare no competing interests.

References

Abiye EO (2016) Atmospheric ventilation corridors and coefficients for pollution plume released from an Industrial Facility in Ile-Ife Suburb, Nigeria. Afr J Environ Sci Technol 10. https://doi.org/10.5897/AJEST2016.2128

Athukorala D, Murayama Y (2021) Urban heat island formation in greater Cairo: spatio-temporal analysis of daytime and nighttime land surface temperatures along the urban–rural gradient. Remote Sens 13:1396. https://doi.org/10.3390/rs13071396

Berger C, Rosentreter J, Voltersen M et al (2017) Spatio-temporal analysis of the relationship between 2D/3D urban site characteristics and land surface temperature. Remote Sens Environ 193:225–243. https://doi.org/10.1016/j.rse.2017.02.020

Buccolieri R, Hang J (2019) Recent advances in urban ventilation assessment and flow modelling. Atmosphere 10. https://doi.org/10.3390/atmos10030144

Cao A, Li Q, Meng Q (2015) Effects of orientation of urban roads on the local thermal environment in Guangzhou City. Procedia Eng 121. https://doi.org/10.1016/j.proeng.2015.09.209

Chen SL, Lu J, Yu WW (2017) A quantitative method to detect the ventilation paths in a mountainous urban city for urban planning: a case study in Guizhou, China. Indoor Built Environ 26:422–437. https://doi.org/10.1177/1420326X15626233

Coccia M (2021) How do low wind speeds and high levels of air pollution support the spread of COVID-19? Atmos Pollut Res 12:437–445. https://doi.org/10.1016/j.apr.2020.10.002

DESA (2019) World population prospects 2019 highlights. online: https://populaAvailabletion.un.org/wpp/Publications/Files/WPP2019_Highlights.pdf. Accessed 15 Dec 2020

Eldesoky AHM, Colaninno N, Morello E (2020) Mapping urban ventilation corridors and assessing their impact upon the cooling effect of greening solutions. https://doi.org/10.5194/isprs-archives-XLIII-B4-2020-665-2020

Fang Y, Gu K, Qian Z et al (2021) Performance evaluation on multi-scenario urban ventilation corridors based on least cost path. J Urban Manag 10:3–15. https://doi.org/10.1016/j.jum.2020.06.006

Franchesca G, Tomohito M, Hikari S, Akira K (2019) Evaluating the use of ventilation efficiency indices to improve urban ventilation. Osaka University;Osaka University;Osaka University, Osaka University

George X, Hua S, Roger A, et al (2021) The effects of urban land cover dynamics on urban heat Island intensity and temporal trends. GIScience & Remote Sensing 58:. https://doi.org/10.1080/15481603.2021.1903282

Giridharan R, Ganesan S, Lau SSY (2004) Daytime urban heat island effect in high-rise and high-density residential developments in Hong Kong. Energy Build 36:525–534. https://doi.org/10.1016/j.enbuild.2003.12.016

Guo F, Zhang H, Fan Y et al (2018) Detection and evaluation of a ventilation path in a mountainous city for a sea breeze: the case of Dalian. Build Environ 145:177–195. https://doi.org/10.1016/j.buildenv.2018.09.010

He B-J (2018) Potentials of meteorological characteristics and synoptic conditions to mitigate urban heat island effects. Urban Climate 24:26–33. https://doi.org/10.1016/j.uclim.2018.01.004

He B-J, Ding L, Prasad D (2020) Wind-sensitive urban planning and design: precinct ventilation performance and its potential for local warming mitigation in an open midrise gridiron precinct. J Build Eng 29:101145. https://doi.org/10.1016/j.jobe.2019.101145

Hou C, Hou J, Kang Q, et al (2018) Research on urban park design combined with the urban ventilation system. Energy Procedia 152. https://doi.org/10.1016/j.egypro.2018.09.139

Jamei E, Ossen DR, Seyedmahmoudian M et al (2020) Urban design parameters for heat mitigation in tropics. Renew Sust Energ Rev 134:110362. https://doi.org/10.1016/j.rser.2020.110362

Jiang Y, Wu C, Teng M (2020) Impact of residential building layouts on microclimate in a high temperature and high humidity region. Sustainability 12:1046. https://doi.org/10.3390/su12031046

Jun Y, Jiayi R, Dongqi S, et al (2021) Understanding land surface temperature impact factors based on local climate zones. Sustain Cities Soc 69https://doi.org/10.1016/j.scs.2021.102818

Lai D, Liu W, Gan T et al (2019) A review of mitigating strategies to improve the thermal environment and thermal comfort in urban outdoor spaces. Sci Total Environ 661:337–353. https://doi.org/10.1016/j.scitotenv.2019.01.062

Li C, Wu K, Wu J (2018) Urban land use change and its socio-economic driving forces in China: a case study in Beijing, Tianjin and Hebei region. Environ Dev Sustain 20:1405–1419. https://doi.org/10.1007/s10668-017-9928-6

Li N, Yang J, Qiao Z et al (2021a) Urban thermal characteristics of local climate zones and their mitigation measures across cities in different climate zones of China. Remote Sens 13:1468. https://doi.org/10.3390/rs13081468

Li X, Stringer LC, Dallimer M (2021b) The spatial and temporal characteristics of urban heat island intensity: implications for East Africa's Urban Development. Climate 9:51. https://doi.org/10.3390/cli9040051

Liu W, Zhang G, Jiang Y, Wang J (2021) Effective range and driving factors of the urban ventilation corridor effect on urban thermal comfort at unified scale with multisource data. Remote Sens 13:1783. https://doi.org/10.3390/rs13091783

Liu Y, Fang X, Cheng C et al (2016) Research and application of city ventilation assessments based on satellite data and GIS technology: a case study of the Yanqi Lake Eco-city in Huairou District, Beijing. Meteorol Appl 23:320–327. https://doi.org/10.1002/met.1557

Luo X, Yang J, Sun W, He B (2021) Suitability of human settlements in mountainous areas from the perspective of ventilation: a case study of the main urban area of Chongqing. J Clean Prod 310:127467. https://doi.org/10.1016/j.jclepro.2021.127467

Ma Y, Zhao M, Li J et al (2021) Cooling effect of different land cover types: a case study in Xi'an and Xianyang. China Sustain 13:1099. https://doi.org/10.3390/su13031099

Min M, Zhao H, Miao C (2018) Spatio-temporal evolution analysis of the urban heat island: a case study of Zhengzhou City. China Sustain 10:1992. https://doi.org/10.3390/su10061992

Schreurs MA (2008) From the bottom up: local and subnational climate change politics. J Environ Dev 17.https://doi.org/10.1177/1070496508326432

Mohajerani A, Bakaric J, Jeffrey-Bailey T (2017) The urban heat island effect, its causes, and mitigation, with reference to the thermal properties of asphalt concrete. J Environ Manage 197:522–538. https://doi.org/10.1016/j.jenvman.2017.03.095

Ngarambe J, Joen SJ, Han C-H, Yun GY (2021) Exploring the relationship between particulate matter, CO, SO2, NO2, O3 and urban heat island in Seoul Korea. J Hazard Mater 403:123615. https://doi.org/10.1016/j.jhazmat.2020.123615

Oke TR, G M, A C, J.A V (2017) Urban climates. In: Chapter 7 Urban Heat Island. Cambridge University Press, pp197–199

Peng Y, Gao Z, Buccolieri R, Ding W (2019) An investigation of the quantitative correlation between urban morphology parameters and outdoor ventilation efficiency indices. Atmosphere 10:33. https://doi.org/10.3390/atmos10010033

Qiao Z, Tian G, Xiao L (2013) Diurnal and seasonal impacts of urbanization on the urban thermal environment: a case study of Beijing using MODIS data. ISPRS J Photogramm Remote Sens 85:93–101. https://doi.org/10.1016/j.isprsjprs.2013.08.010

Qiao Z, Xu X, Wu F et al (2017) Urban ventilation network model: a case study of the core zone of capital function in Beijing metropolitan area. J Clean Prod 168:526–535. https://doi.org/10.1016/j.jclepro.2017.09.006

Qin H, Lin P, Lau SSY, Song D (2020) Influence of site and tower types on urban natural ventilation performance in high-rise high-density urban environment. Build Environ 179.https://doi.org/10.1016/j.buildenv.2020.106960

Qin Z, Karnieli A, Berliner P (2001) A mono-window algorithm for retrieving land surface temperature from Landsat TM data and its application to the Israel-Egypt border region. Int J Remote Sens 22.https://doi.org/10.1080/01431160010006971

Qiquan Y, Xin H, Jie Y, Yue L (2021) The relationship between land surface temperature and artificial impervious surface fraction in 682 global cities: spatiotemporal variations and drivers. Environ Res Lett 16.https://doi.org/10.1088/1748-9326/abdaed

Ramponi R, Blocken B, de Coo LB, Janssen WD (2015) CFD simulation of outdoor ventilation of generic urban configurations with different urban densities and equal and unequal street widths. Build Environ 92:152–166. https://doi.org/10.1016/j.buildenv.2015.04.018

Ren C, Yang R, Cheng C et al (2018) Creating breathing cities by adopting urban ventilation assessment and wind corridor plan - the implementation in Chinese cities. J Wind Eng Ind Aerodyn 182:170–188. https://doi.org/10.1016/j.jweia.2018.09.023

Ren J, Yang J, Zhang Y, et al (2022) Exploring thermal comfort of urban buildings based on local climate zones. J Clean Prod 130744.https://doi.org/10.1016/j.jclepro.2022.130744

Roxon J, Ulm F-J, Pellenq RJ-M (2020) Urban heat island impact on state residential energy cost and CO 2 emissions in the United States. Urban Climate 31. https://doi.org/10.1016/j.uclim.2019.100546

Shi Y, Yan Z, Li C, Li C (2021) Energy consumption and building layouts of public hospital buildings: a survey of 30 buildings in the cold region of China. Sustain Cities Soc 74:103247. https://doi.org/10.1016/j.scs.2021.103247

Stewart ID, Oke TR (2012) Local climate zones for urban temperature studies. Bull Am Meteor Soc 93:1879–1900. https://doi.org/10.1175/BAMS-D-11-00019.1

Tan Z, Lau KK-L, Ng E (2016) Urban tree design approaches for mitigating daytime urban heat island effects in a high-density urban environment. Energy Build 114:265–274. https://doi.org/10.1016/j.enbuild.2015.06.031

Tian R, Weiqi Z, Jia W (2021) Beyond intensity of urban heat island effect: a continental scale analysis on land surface temperature in major Chinese cities. Sci Total Environ 791.https://doi.org/10.1016/j.scitotenv.2021.148334

Trihamdani A, Lee H, Kubota T, Phuong T (2015) Configuration of green spaces for urban heat island mitigation and future building energy conservation in Hanoi Master Plan 2030. Buildings 5.https://doi.org/10.3390/buildings5030933

Wang Z, Meng Q, Allam M et al (2021) Environmental and anthropogenic drivers of surface urban heat island intensity: a case-study in the Yangtze River Delta China. Ecol Indic 128:107845. https://doi.org/10.1016/j.ecolind.2021.107845

Wong MS, Nichol JE, To PH, Wang J (2010) A simple method for designation of urban ventilation corridors and its application to urban heat island analysis. Build Environ 45:1880–1889. https://doi.org/10.1016/j.buildenv.2010.02.019

Xie P, Yang J, Sun W et al (2022) Urban scale ventilation analysis based on neighborhood normalized current model. Sustain Cities Soc 80:103746. https://doi.org/10.1016/j.scs.2022.103746

Xu Y, Ren C, Ma P et al (2017) Urban morphology detection and computation for urban climate research. Landsc Urban Plan 167:212–224. https://doi.org/10.1016/j.landurbplan.2017.06.018

Xu Y, Wang W, Chen B et al (2021) Identification of ventilation corridors using backward trajectory simulations in Beijing. Sust Cities Soc 70:102889. https://doi.org/10.1016/j.scs.2021.102889

Yang J, Jin S, Xiao X et al (2019a) Local climate zone ventilation and urban land surface temperatures: towards a performance-based and wind-sensitive planning proposal in megacities. Sustain Cities Soc 47:101487. https://doi.org/10.1016/j.scs.2019.101487

Yang J, Wang Y, Xiao X et al (2019b) Spatial differentiation of urban wind and thermal environment in different grid sizes. Urban Climate 28:100458. https://doi.org/10.1016/j.uclim.2019.100458

Yang J, Zhan Y, Xiao X et al (2020) Investigating the diversity of land surface temperature characteristics in different scale cities based on local climate zones. Urban Climate 34:100700. https://doi.org/10.1016/j.uclim.2020.100700

Yang J, Yang Y, Sun D et al (2021) Influence of urban morphological characteristics on thermal environment. Sustain Cities Soc 72:103045. https://doi.org/10.1016/j.scs.2021.103045

Yunlong P, Zhi G, Riccardo B, et al (2021) Urban ventilation of typical residential streets and impact of building form variation. Sustain Cities Soc 67.https://doi.org/10.1016/j.scs.2021.102735

Zhang Y, Cheng J (2019) Spatio-temporal analysis of urban heat island using multisource remote sensing data: a case study in Hangzhou, China. IEEE J Sel Top Appl Earth Observations Remote Sensing 12:3317–3326. https://doi.org/10.1109/JSTARS.2019.2926417

Zhao Z, Shen L, Li L et al (2020) Local climate zone classification scheme can also indicate local-scale urban ventilation performance: an evidence-based study. Atmosphere 11:776. https://doi.org/10.3390/atmos11080776

Zhang Y, Zhang X, Xu W, Jiao B (2021) A case study on urban ventilation assessment with local climate zone (LCZ) parameters. IOP Conf Ser: Earth Environ Sci 696:012033. https://doi.org/10.1088/1755-1315/696/1/012033